Quaternary Geochronology 74 (2023) 101421

Contents lists available at ScienceDirect

Quaternary Geochronology

journal homepage: www.elsevier.com/locate/quageo

# Evidences of the Blake and Iceland Basin magnetic excursions in southeastern Iberia and chronological implications for the Padul sedimentary record

Luis Valero [a,b,1,*], Antonio García-Alix [c,d], Gonzalo Jiménez-Moreno [c], Jon Camuera [d,e], Alejandro López-Avilés [c], María J. Ramos-Román [e], Francisco J. Jiménez-Espejo [d], Elisabet Beamud [a], Estefanía Maestre [a], R. Scott Anderson [f]

[a] Laboratori de Paleomagnetisme, Geosciences Barcelona CCiTUB-CSIC, Barcelona, Spain
[b] Department of Earth Sciences, University of Geneva, Switzerland
[c] Departamento de Estratigrafía y Paleontología, Universidad de Granada, Spain
[d] Instituto Andaluz de Ciencias de La Tierra (CSIC-UGR), Armilla, Spain
[e] Department of Geosciences and Geography, University of Helsinki, Finland
[f] School of Earth and Sustainability, Northern Arizona University, Flagstaff, AZ, USA

ARTICLE INFO

*Keywords:*
Paleoclimate
Magnetic excursion
Blake
Iceland Basin
Padul
Mediterranean paleoclimate

ABSTRACT

The Padul-15-05 sediment core provides an exceptional perspective of the paleoenvironmental and climate change in the Western Mediterranean region for the last *ca.* 200 kyr. However, even though a robust chronology mainly relying on radiometric dating is available for the last 50 ka, the chronology for the older sediments is not yet fully resolved. Ages for the bottom part of the core (>21 m) were previously inferred from amino-acid racemization dating and sediment accumulation rates. In this work, we provide a more accurate chronology for the older part (>100 kyr) of the Padul-15-05 sediment core record based on the recognition of past Earth's magnetic excursions. We identify an interval prone of reversed polarity samples close to MIS-5e/5 d transition that we correlate to the Blake geomagnetic excursion (116.5 kyr–112 kyr). In addition, we identify an interval of low inclinations and two reversed samples that we interpret as the Iceland Basin geomagnetic excursion (192.7 kyr–187.7 kyr: *wide* scenario of VGP <40°). Our new results, which include IRM acquisition curves that contribute to understand the magnetic mineralogy, enhances the robustness of the age model for the Padul-15-05 sedimentary sequence by adding an independent age dataset with new accurate tie-points. Our refined age control together with the available paleoenvironmental and paleoclimate multiproxy data provide insightful information to unveil the response of the western Mediterranean environments to regional environmental and climate change.

## 1. Introduction

The Padul wetland, located in SE Spain (Fig. 1), preserves a long and continuous sedimentary and paleoenvironmental record of the last ~1 Ma (Ortiz et al., 2004). For decades, it has been considered an extraordinary and unique paleoenvironmental and paleoclimatic archive in the Iberian Peninsula (Menéndez-Amor and Florchütz, 1962; Pons and Reille, 1988; Ortiz et al., 2004; Camuera et al., 2018, 2019), containing one of the few long and continuous sedimentary records (>100 kyr) from southwestern Europe and the Mediterranean region. The Padul paleoenvironmental data provides an opportunity to assess the climatic evolution of the critical Mediterranean zone, valuable to constrain predictive climate models (Pancost, 2017). Several sedimentary cores have been taken in this area during the last 50 years; however, the development of an accurate chronology has been a critical issue, especially beyond the range of the radiocarbon dating (Menéndez-Amor and Florchütz, 1962; Pons and Reille, 1988; Ortiz et al., 2004; Camuera et al., 2018).

* Corresponding author. Department of Earth Sciences, University of Geneva, Switzerland.
*E-mail address:* lvalero@geo3bcn.csic.es (L. Valero).
[1] Present address: Laboratori de Paleomagnetisme, Geosciences Barcelona CCiTUB-CSIC, Barcelona, Spain.

https://doi.org/10.1016/j.quageo.2022.101421
Received 29 July 2022; Received in revised form 5 December 2022; Accepted 5 December 2022
Available online 7 December 2022

Among all the available records, here we focus on the Padul-15-05 core, which has provided key insights on the environmental evolution of a Mediterranean wetland area during the last two glacial-interglacial climate cycles, based on lithological characterization, element geochemistry analysis (Ramos-Román et al., 2018a, 2018b; Camuera et al., 2018), lipid biomarkers (García Alix et al., 2021; Rodrigo-Gámiz et al., 2022) and detailed palynological analyses (Ramos-Román et al., 2018a, 2018b; Camuera et al., 2019, 2021, 2022).

An accurate chronology is available for the Padul-15-05 core for sediments younger than 50 kyr based on radiocarbon dating. However, the chronology for older intervals is yet uncertain (Camuera et al., 2018) and only is based on ages derived from amino acid racemization (AAR) in mollusk shells, which lead to large uncertainty in ages of up to ±30 kyr, and from sedimentary accumulation rates estimated for the different sedimentary facies (Camuera et al., 2018).

In this work, we explore the record of geomagnetic excursions, short-lived episodes when Earth's magnetic field deviates into an intermediate polarity state (Roberts, 2008), that can provide useful chronological information (Tucholka et al., 1987). The occurrence of Earth's geomagnetic excursions in the Padul-15-05 core could provide precise age constraints in sediments older that the high-resolution radiocarbon interval (*i.e.* older than *ca.* 50 kyr BP). We aim to investigate magnetic polarity of an interval close to the end of the MIS-5e/5 d transition in the Padul-15-05 record, that would contain the Blake geomagnetic excursion (112 kyr–125 kyr; Laj and Channell, 2007). In addition, we investigate the presence of the Iceland Basin geomagnetic excursion (midpoints of the excursion in the 192 - 189 kyr range; Channell et al., 2014) close to the interpreted MIS-7/6 boundary. These well-known excursions could provide time constraints to build a more accurate dating of a precious paleoenvironmental archive, bringing out new insights on the implications of climate change on the Western Mediterranean area.

To test the occurrence of geomagnetic excursions in the Padul-15-05 record, we first assessed the magnetic carriers by means of isothermal remanent magnetization (IRM) acquisition for all the facies represented in the studied interval. After a positive determination of the suitability of magnetic mineralogy to carry out alternate field (AF) demagnetization, we then demagnetized, and interpreted the magnetic inclination for a set of 101 samples throughout the lower part of the core (below 21 m depth) focusing on the expected position for the targeted excursions (Blake and Iceland Basin, Fig. 2). We present the IRM acquisition results and the demagnetization results. We show that there is an interval prone of reversed polarity samples occurring during the climatostratigraphically and paleoenvironmentally constrained MIS-5e/5 d transition, that we identify as the Blake geomagnetic excursion. In addition, an interval with reversed and low magnetic inclinations at the base of the core is here interpreted as the Iceland Basin geomagnetic excursion. Based on this new age constraints, we present a new chronology for the Padul-15-05 record.

## 2. Geological setting of the padul wetland

The Padul wetland is located at the foothill of the Sierra Nevada range (South Iberian Peninsula), at 726 m above sea level, in the small (45 km$^2$) NW-SE elongated Padul-Niguelas extensional endorheic basin. The Sierra Nevada is an E-W aligned alpine mountain chain, located in the Internal Zone of the Betic Cordillera, with elevation ranging between *ca.* 900–3479 m above sea level. Despite its meridional location, its high topography sustained glacial conditions during the cold phases of the Late Pleistocene (Schulte, 2002). However, due to its southernmost location and the nearby Mediterranean Sea influence, Late Pleistocene valley glaciers occurred at higher elevation in Sierra Nevada than in other mountain ranges of the Iberian Peninsula (Gómez-Ortiz et al., 2005). Valley glaciers extended down to *ca.* 2000–2100 m on north-facing slopes and to *ca.* 2400–2500 m on south-facing slopes during the Late Pleistocene (Palacios et al., 2016). The sedimentary archive of the Padul wetland registered continuous lacustrine and peatland sedimentation during the last 1 Ma, which made this wetland an environmental refuge for cold faunas during extreme climatic events (Álvarez Lao et al., 2009; García-Alix et al., 2012).

Previous cores from the Padul wetland (Menéndez-Amor and Florschutz, 1964; Florschutz et al., 1971; Pons and Reille, 1988; Ortiz et al., 2004) present different sediment thickness and sedimentation rates depending on their proximity to the depocenter of the basin, located

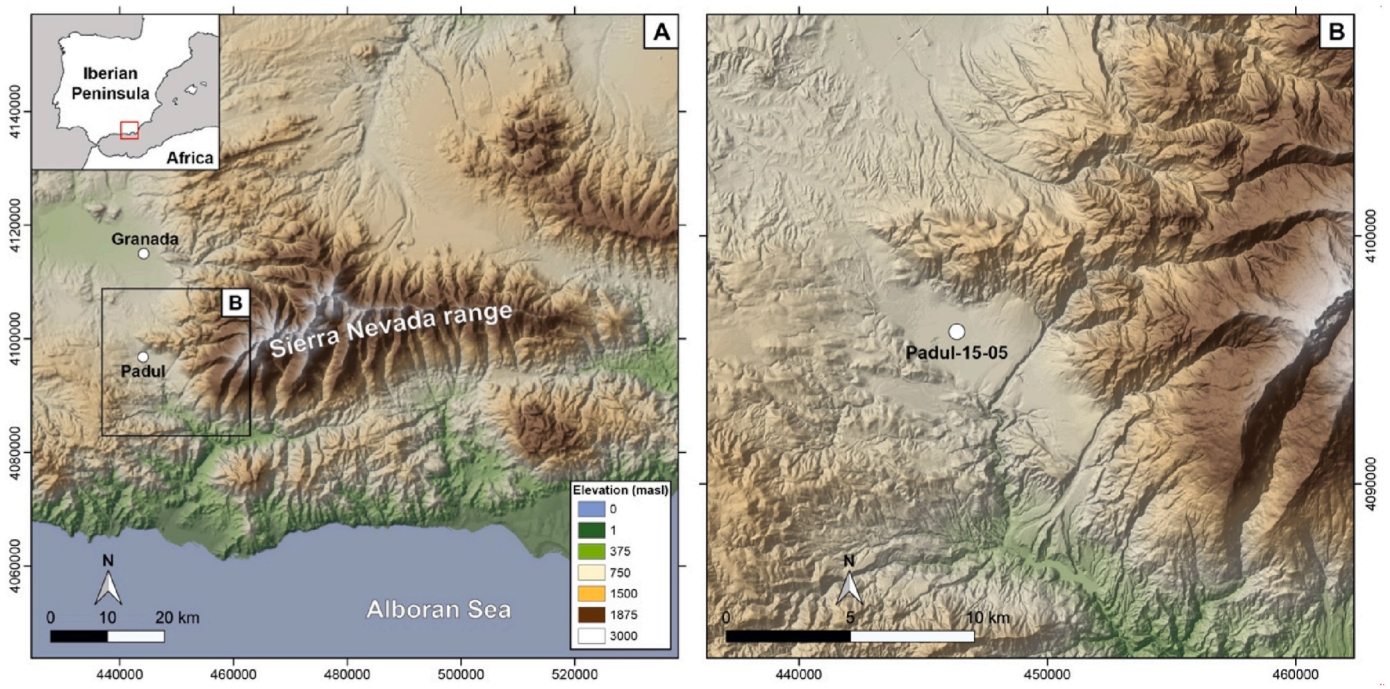


**Fig. 1.** (A) Geographical location of the Padul study site at the foothill of the Sierra Nevada Range, SE Spain. On the right, (B) a more detailed location of the Padul-15-50 core record.

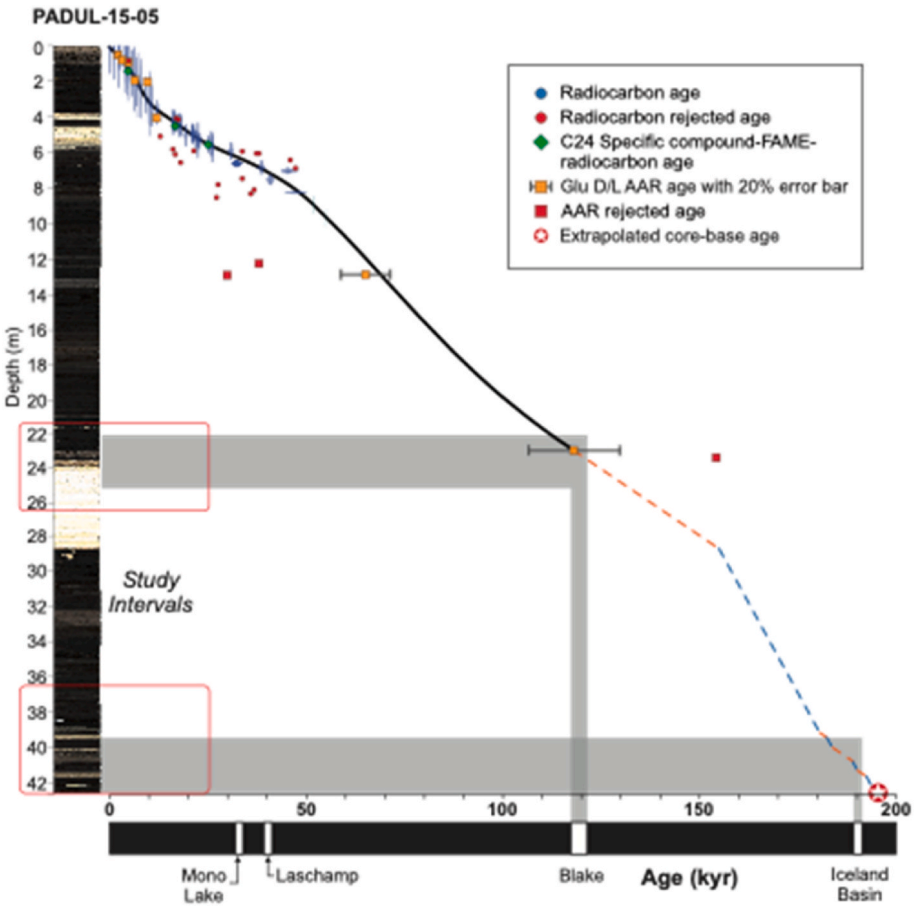


**Fig. 2.** The Padul-15-05 core and the available chronology based on radiometric and amino acid racemization dating (Camuera et al., 2018). Red squares mark our intervals of study. Orange dashed lines represent the extrapolated age following the calculated sedimentation rate for carbonate facies (Camuera et al., 2018). Blue dashed lines represent the extrapolated age following the calculated sedimentation rate for peat facies (Camuera et al., 2018). The grey stripes show the potential position of the Blake and Iceland Basin magnetic excursions following the last age model available in the Padul 15–05 core (Camuera et al., 2018). Ages for the magnetic excursions come from in Laj and Channell (2007).

near the main Padul-Niguelas fault at the NE edge of the basin (Domingo-García et al., 1983). Here we study the Padul-15-05 core (37°00′39″ N, 3°36'°14″ W), which was drilled in July 2015, at around 50 m from the current edge of the Padul lake. A continuous core was retrieved using a Rolatec RL-48-L hydraulic piston coring machine from the Centre for Scientific Instrumentation of the University of Granada. Drilling ended at 42.64 m depth when conglomerates were found, precluding further coring.

### 2.1. Sedimentary facies

The lithology of the Padul-15-05 in the core interval studied here (41.71 m–21 m), begins with peat sediments at the bottom (42.64 m depth) up to 28.78 m depth. Three thin marl layers are interbedded at 41.71–41.38 m, 40.81–40.24 m and 39.52–39.33 m depth, whilst a thin clay layer is found at 33.22–32.35 m depth. Marls predominate from 28.78 m to 25.44 m, transitioning to carbonate sediments up to 23.57 m depth. From 23.57 m to 5.98 m depth lithology is mainly composed of peat (Fig. 2). Ten thin dolomitic layers with maximum thickness of 7 cm (each layer) are randomly distributed in the study interval at 40.22, 39.29, 39.05, 38.83, 32.31, 23.58, 23.47, 22.75, 22.49, and 21.71 m depth.

### 2.2. Age model

In this section, we focus on the Padul-15-05 record (Ramos Román et al., 2018a, 2018b; Camuera et al., 2018; 2019; 2021) since previous records of the wetland lack an accurate age control (Nestares and Torres, 1998; Ortiz et al., 2004, 2010; Torres et al., 2020). The age-depth model of the Padul-15-05 record (Ramos-Román et al., 2018a; 2018b; Camuera et al., 2018, 2019, 2021) was obtained from 48 AMS radiocarbon dates (including 3 compound specific radiocarbon dates) and 4 of amino acid racemization (AAR) dates from mollusk shells (Fig. 2). In this core, there are only two dates older than 50 kyr, which yielded ~68 and ~117 kyr at 13.13 and 23.39 m depth, respectively, and age tie-points are lacking below that depth. For the lower part of the core, inferred sediment accumulation rates (SAR) and a cyclostratigraphic analysis of multi-proxy data suggest that the core preserves a continuous record of the last ~197 kyr (from late MIS-7 up to the present) (Camuera et al., 2018, 2019, 2021, Fig. 2). Accordingly, we focused our analysis on the bottom part of the core, between 42.64 and 21 m, which would correspond to a duration of ~104 kyr based on the Camuera et al. (2018) chronology (Fig. 2).

## 3. Methods

### 3.1. Sampling

The Padul-15-05 core is stored at 4 °C in the sediment core repository of the Department of Stratigraphy and Paleontology of the University of Granada (Spain). A total of 101 samples were collected from the sediment core in the laboratory. All samples were taken perpendicular to the core in plastic boxes, except for 7 samples that were taken in quartz boxes to perform stepwise thermal demagnetization. In addition, 5 samples were taken in the most characteristic sedimentary facies to carry out magnetic mineralogy analysis based on IRM acquisition. Sampling density varies between 5 cm and 15 cm in the critical sampling intervals (Drive 44, 15 cm; Drive 48, 35 cm; Drive 71, 11 cm; Drive 81, 27 cm; a drive is a part of the core, with variable thickness normally of around 50 cm) avoiding, when possible, organic-rich levels.

### 3.2. Magnetic analysis

Magnetic analyses were carried out at the Paleomagnetic Laboratory of Barcelona (CCiTUB-CSIC). Natural remanent magnetization (NRM) and subsequent analysis of sample magnetization were measured using the cryogenic magnetometer (2-G Enterprises). Before sampling the core, we conducted measurements of the NRM of the empty plastic boxes and only those plastic boxes with NRM values below $3e10^{-8}$ A/m$^2$ selected for sampling. Once sampled, demagnetization was performed using an AF Demagnetizer D-Tech 2000 (ASC Scientific). Step-wise increasing Alternate Fields (AF) were applied in the three-axis directions for each sample upon a significant decay of the NRM intensity, upon samples displayed erratic directions, or up to 120 mT. Demagnetization steps were chosen depending on the NRM intensity. In those samples with NRM intensity values at least $1e10^{-7}$ A/m$^2$ demagnetization steps averaged 15 mT, whilst steps of 2 mT were conducted in samples with lower NRM intensity values. Thermal demagnetization was also performed for 7 samples in quartz boxes. In order to identify the main carriers of the magnetic remanence, acquisition of the isothermal remanent magnetization (IRM) at room temperature was done by means of the Pulse magnetizer ASC IM10-30 (ASC-Scientific) on selected samples previously AF demagnetized. IRM steps were, first, a step in -z of 1200 mT, to apply a maximum field in order to align the random magnetization after AF's, and subsequently steps of (+z) 2, 4, 6, 8, 10, 12.5, 15, 20, 25, 30, 40, 50, 60, 70, 80, 100, 150, 200, 300, 400, 600, 800, 1000 and 1200 (mT). This procedure also implies a backfield analysis and determination of Hc.

## 4. Results

### 4.1. Magnetic mineralogy

We carried out acquisition of the IRM analysis for the whole range of facies present in the samples that underwent demagnetization procedures. These lithologies are dolomitic facies (BL5 at 22.75 m and IB19 at 39.05), organic peat facies (BL9 at 22.92 m), carbonate facies (BL 40 at 24.81 m), and clayey peat (IB 13 at 38.34). IRM acquisition results reveal that a *soft* magnetic mineral is the main magnetic carrier for all samples (Fig. 3), since IRM curves saturate between 200 mT and 400 mT, discarding the presence of *hard* magnetic minerals like hematite or goethite, and Hc depict low values (<50 mT) for all samples except IB19. This sample consists of dolomite facies and shows higher Hc values and higher field saturation, which suggests that there is a relative increase in a *harder* magnetic component. For all samples, our results evidence that magnetic remanence is carried by a low magnetic coercivity mineral, more likely (Ti-)magnetite, although the presence of maghemite cannot be excluded. The magnetic carrier for sample IB19 is probably also magnetite but mixed with a *harder* component. The revealed predominance of *soft* magnetic carriers ensures that AF demagnetization is an appropriate technique to correctly isolate the characteristic components of the studied samples.

Nevertheless, stepwise thermal demagnetization was also tested in seven specimens in quartz boxes. Lithologies that underwent thermal demagnetization are peat (BL25 at 23.10 cm, BL16 at 23.20 cm) and carbonate (BL19 at 23.27 cm; BL 21 at 23.31 cm; BL 23 at 23.36 cm; and BL38 at 24.6 cm). Erratic directions appear at low temperatures, normally between 200°C and 250 °C (in Fig. 4, BL-21), which is interpreted

| Sample | Depth (m) | Lithology |
|---|---|---|
| BL5 | 22.7 | Dolomite |
| BL9 | 22.93 | Peat |
| BL40 | 24.81 | Carbonate |
| IB13 | 38.34 | Clayey peat |
| IB19 | 39.02 | Dolomite |

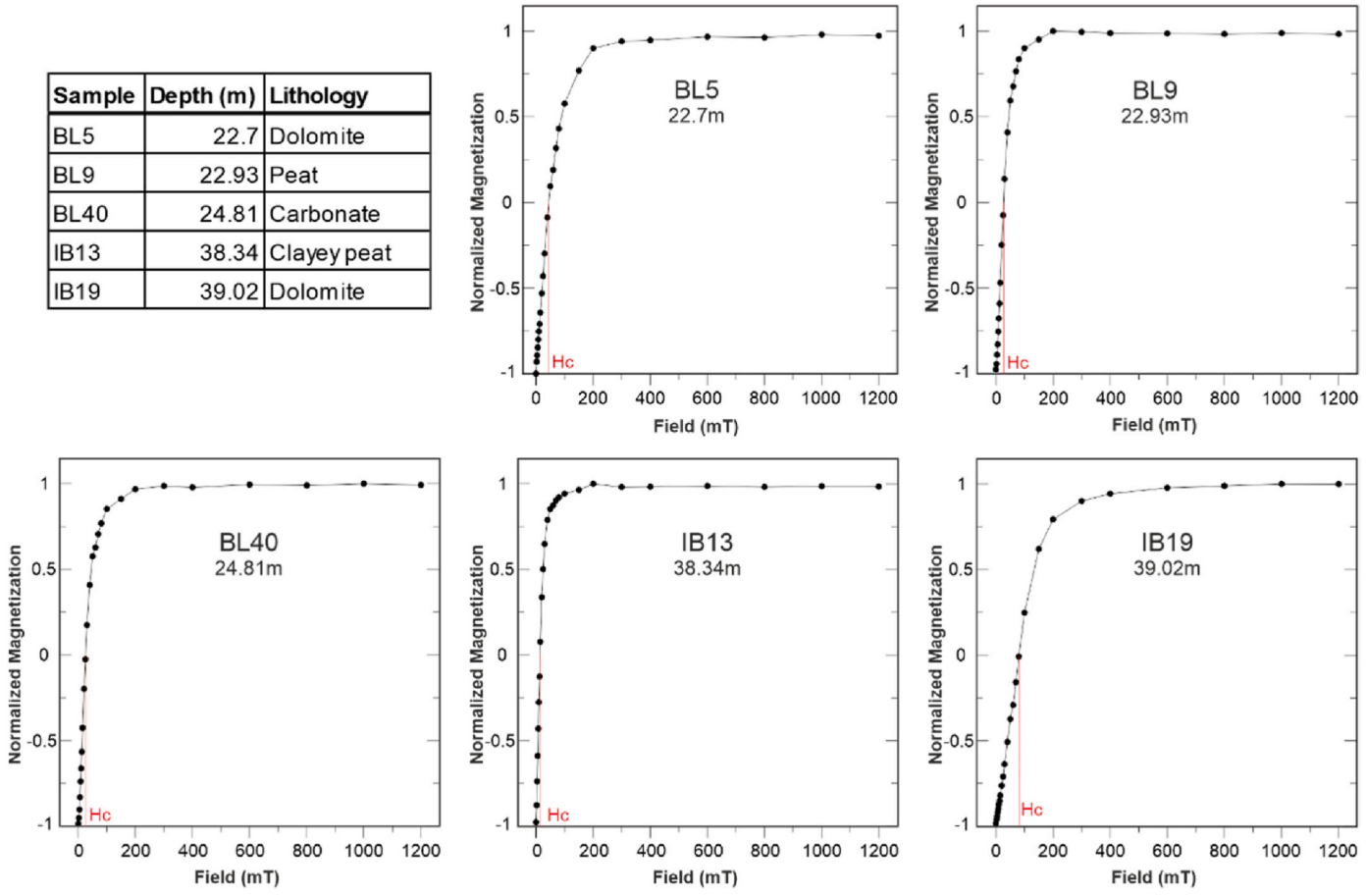


**Fig. 3.** Acquisition of the IRM curves for five representative samples. The similarity between IRM curves reveal small differences in magnetic carriers; all of them depict a relatively low field saturation, which points towards magnetite as the main magnetic carrier. Hc: Coercivity.

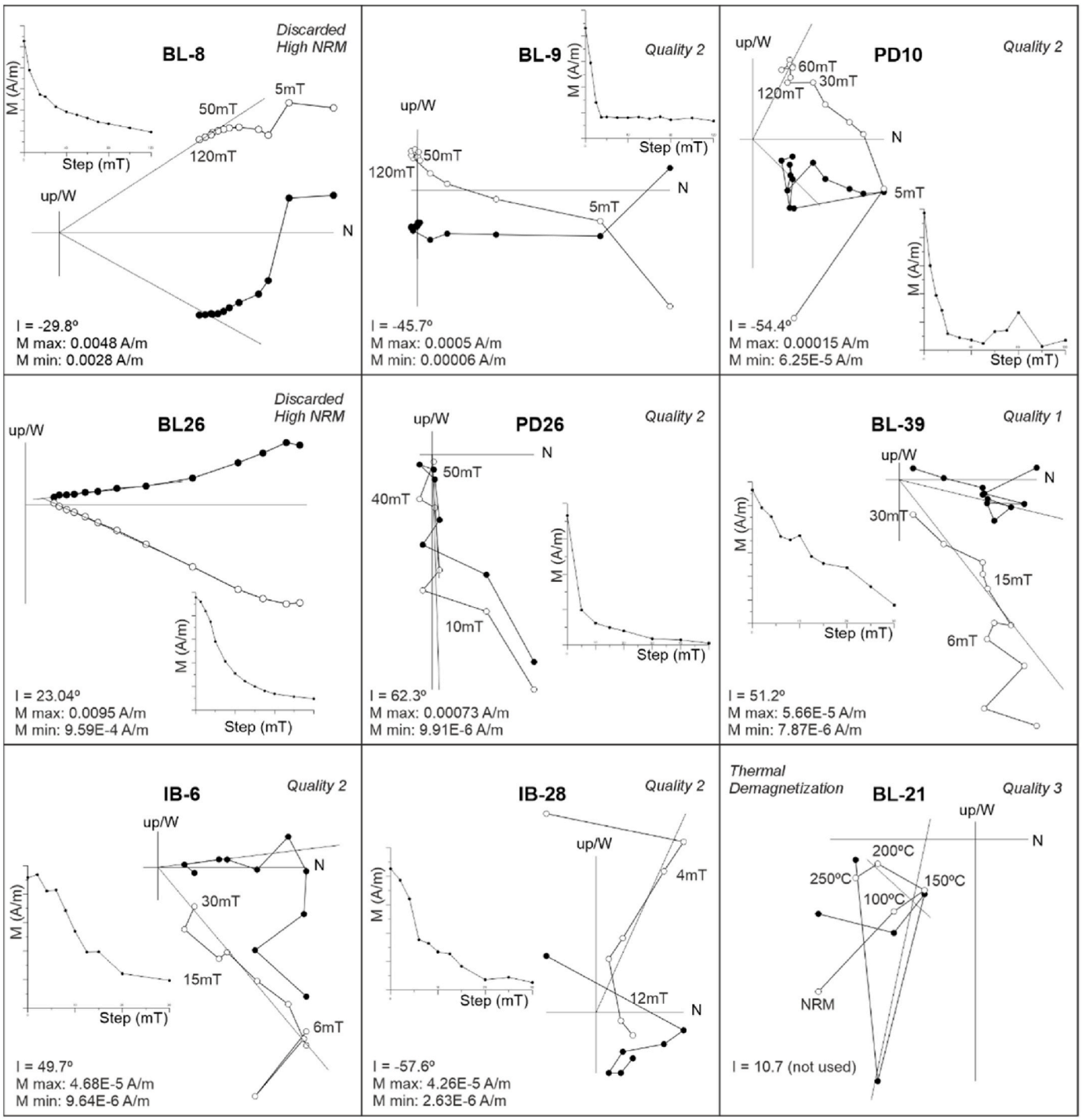


**Fig. 4.** Demagnetization diagrams of characteristic samples. All the samples are interpreted as of normal polarity with positive inclinations (white dots) except for BL-9, PD-10 and IB-28, which are interpreted as samples of reversed polarity. Sample BL-8 show high coercivity minerals and a non-complete demagnetization, and is discarded for defining a magnetic polarity. Also discarded is sample BL-21, which underwent thermal demagnetization, and depict a non-reliable direction.

as a result of sulfide transformation into magnetite during the heating process.

### 4.2. Natural remanent magnetization

NRM values range between 10 and 1500 e10$^{-6}$A/m along the core. There are some outliers with very high NRM values (>5000 e10$^{-6}$A/m) represented by BL8, BL 26, PD 34, IB31, IB32, and IB42 (Figs. 4–6). These samples were discarded for magnetic polarity interpretation due to their anomalous high values. Some of these samples do not show the viscous component and depict a straight decay to the origin during progressive demagnetization (BL26). Other samples show a non-complete demagnetization likely related to the occurrence of a high coercivity magnetic carrier (BL8, Fig. 4) that resisted AF demagnetization. Other samples show an ordinary behavior (PD34, IB31, IB32, IB42), but due to their high NRM, we did not consider them for polarity interpretation. There is no link between intervals of high magnetic susceptibility and samples with anomalously high NRM intensity values (Figs. 5 and 6).

There is a correlation between certain facies and magnetic

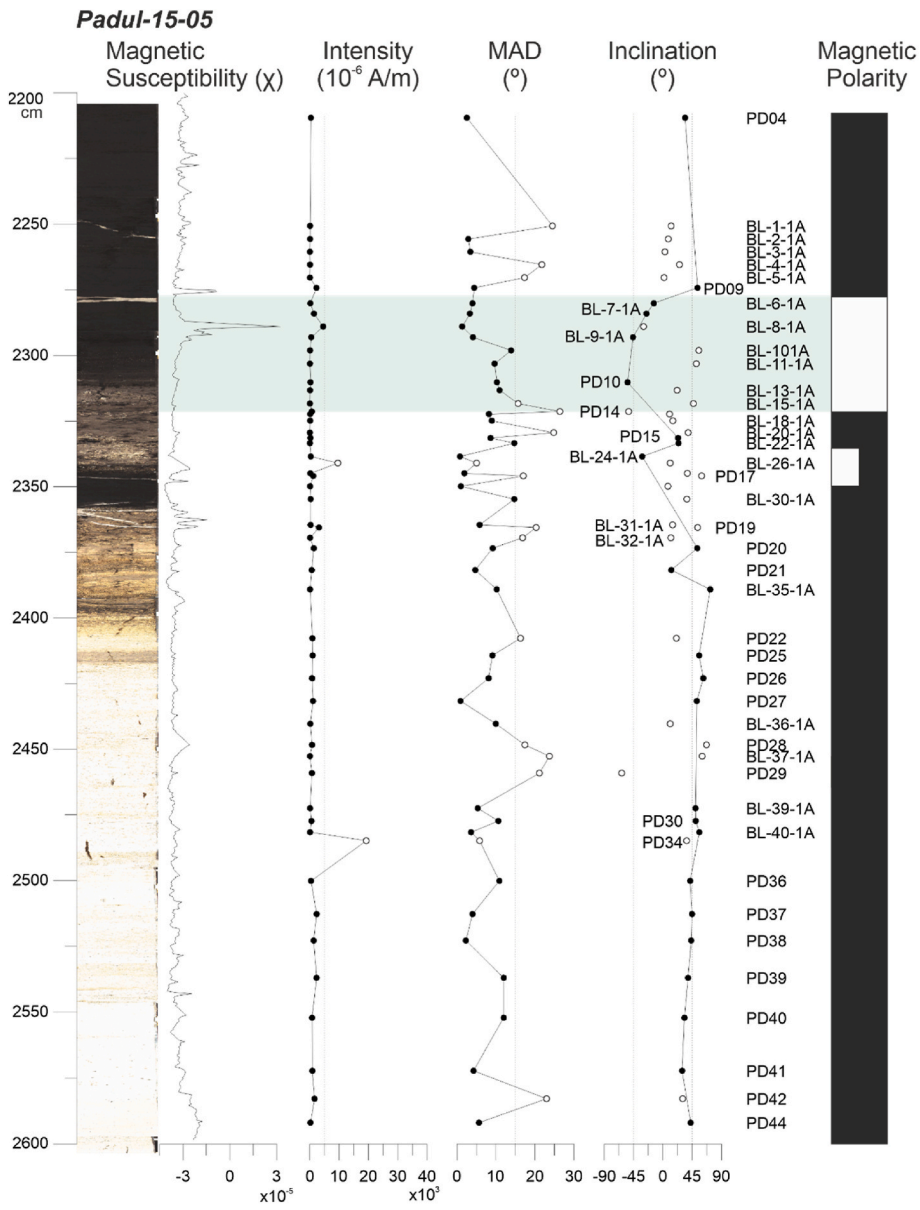


**Fig. 5.** Demagnetization results for the interval of the Padul-15-05 core ranging from 2600 cm to 2200 cm depth. From left to right: picture of the core record, bulk magnetic susceptibility (Camuera et al., 2018), NRM intensity, MAD angles, inclination values, and the interpreted polarity from inclination results (black areas mark normal polarity intervals and white reversed polarity). White-filled dots in the intensity and MAD columns are discarded for polarity analysis due to their high intensity or MAD values > 15°. The rest of white filled dots in the inclination column represent low quality samples, and have been discarded for magnetic polarity interpretation. The grey strip marks the area of anomalous polarity, here interpreted as the main body of the Blake event. Inclinations between −45° and 45° are considered transitional.

susceptibility, specially between light-brown carbonate facies and clay facies, which have higher magnetic susceptibility (Camuera et al., 2018). Principal component analysis results including element geochemical data obtained by X-ray Fluorescence scanner and magnetic susceptibility also reveal a positive correlation of magnetic susceptibility with silica and aluminum content.

### 4.3. Magnetic polarity results

A reorientation of the core to correct rotations upon drilling has not been conducted. Hence, magnetic declination is not reconstructed and Virtual Geomagnetic Poles are not available. Polarity results rely on magnetic inclinations. The inclination for most of the samples shows two components. A lower field component, likely a present-day viscous component, that rapidly (after 5 mT–10 mT) changes towards a more stable component that we interpret as the Characteristic direction (ChRM) (Fig. 4). We classified the samples into three qualities depending on their demagnetization trend. In general, lithology does not control sample quality, except in those samples with very high organic matter content, which yield very low intensities and erratic directions and thus lower quality. Class one shows a ChRM direction towards the origin (e.g., PD20, BL39, IB6, Fig. 4), class two samples display a cluster behavior that does not reach the origin (e.g., BL9, PD10) and class three samples are those with uncertain ChRM directions due to a high MAD angle or because they do not show a clear decay towards the origin. The latter were not considered (white circles) for polarity purposes (Figs. 5 and 6). In general, samples show a positive inclination (around 45°) that we interpret as normal polarity (Figs. 5 and 6). Some intervals, however, present negative or very low inclinations, such as the intervals ranging from 2275 cm to 2350 cm depth, 3825 cm–3860 cm, and 3940 cm–4020 cm (shaded areas in green Figs. 5 and 6)

## 5. Discussion

### 5.1. Identification of the blake event

The interpretation of the interval between 2321 and 2277 cm as of reversed polarity is supported by, at least, five samples with negative inclinations, being four of them consecutive (Fig. 5). Furthermore, low quality samples, not included in the main analysis, show negative or

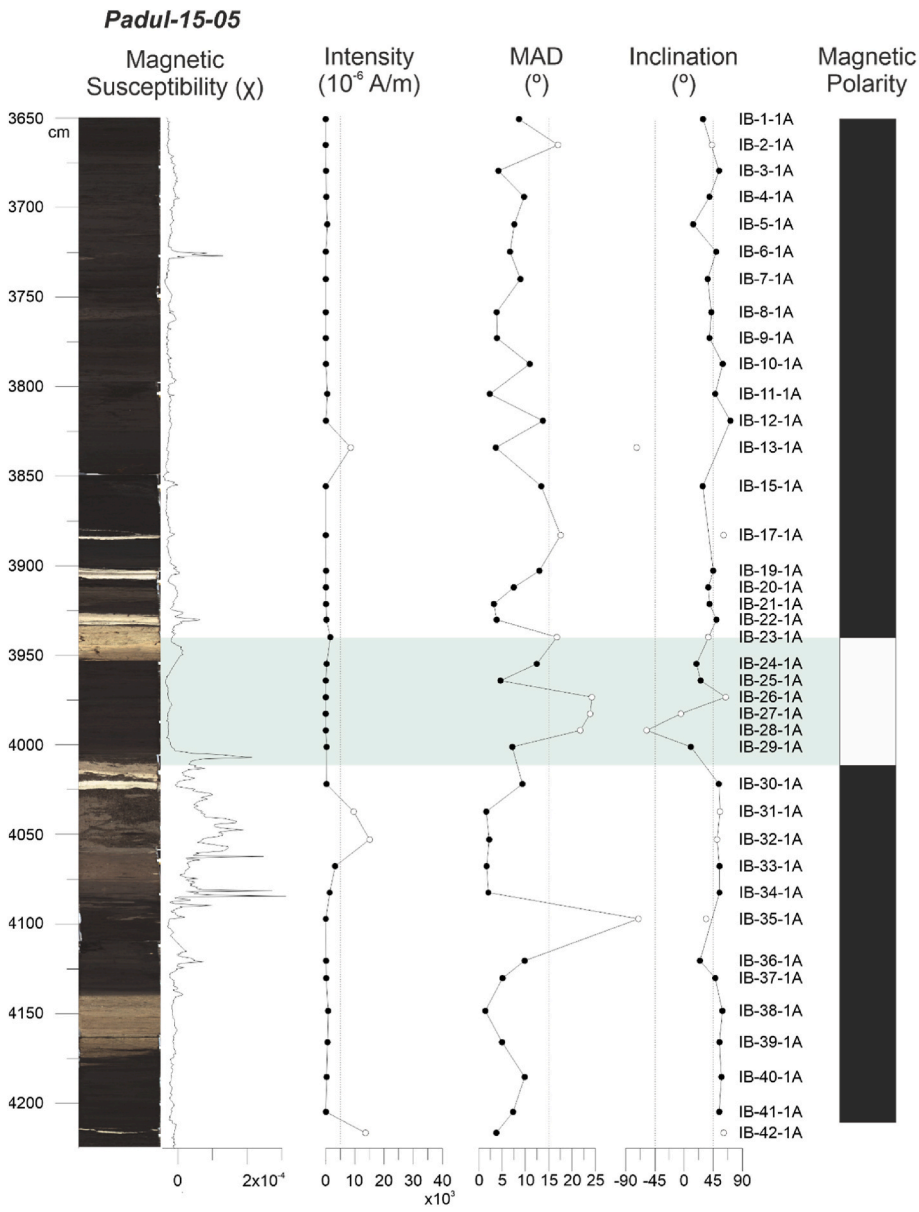


**Fig. 6.** Demagnetization results for the interval of the Padul-15-05 core ranging from 4200 to 3650 cm depth. From left to right: picture of the core record, bulk magnetic susceptibility (Camuera et al., 2018), NRM intensity, MAD angles, inclination values, and the interpreted polarity from inclination results (black marks normal polarity intervals and white reversed polarity). White-filled dots in the intensity and MAD columns are discarded for polarity analysis due to their high intensity or MAD values $> 15°$. The rest of white filled dots in the inclination column represent low quality samples, and have been discarded for magnetic polarity interpretation. The grey strip marks an area of negative inclinations, low quality directions and high MAD angles, interpreted as the Iceland Basin event. Inclinations between $-45°$ and $45°$ are considered transitional.

very low inclinations (Fig. 5). Lithological and palynological changes in this interval evidence a higher relative lake level before *ca.* 2270 cm and warm and wet conditions related to the MIS-5e (Camuera et al., 2018). Additionally, the extrapolation of AAR dates (Camuera et al., 2018) and a cyclostratigraphic analysis of palynological indexes placed the MIS-6/5 transition (*ca.* 128 kyr) at *ca.* 2500 cm (Camuera et al., 2019).

Most of the studies agree in that the Blake geomagnetic event occurs around the MIS-6/5 transition (e.g. Laj and Channell, 2007). The Blake event has been recognized as a global geomagnetic feature, formed by two short periods of almost reverse polarity separated by a short period of almost normal polarity (Laj and Channell, 2007). The Blake excursion has been found in diverse geological archives including marine and loess sediments, caves, stalagmites or volcanic rocks (e.g. Smith and Foster, 1969; Broecker and Van Donk, 1970; Denham and Cox, 1971; Denham, 1976; Creer et al., 1980; Verosub, 1982; Tucholka et al., 1987; An et al., 1991; Tric et al., 1991; Zhu et al., 1994; Fang et al., 1997; Parés et al., 2004; Thouveny et al., 2004; Lund et al., 2006; Laj and Channell, 2007; Bourne et al., 2012; Osete et al., 2012; Channell et al., 2012; Singer et al., 2014). Different ages for this excursion are provided depending on the methodology used (Laj and Channell, 2007). One of the most solid ages for the Blake event is $120 \pm 12$ kyr, based on $^{40}Ar/^{39}Ar$ dating for a lava flow (Singer et al., 2014). Thouveny et al. (2004) suggest an age range for the Blake event between 122 kyr and 115 kyr, coincident with Fang et al. (1997) based on thermoluminescence. Also robust, but slightly younger in age, is the identification of the Blake event in a north Iberian stalagmite record dated using U-series between $116.5 \pm 0.7$ kyr and $112.0 \pm 1.9$ kyr (Osete et al., 2012).

Although it is claimed that the weak magnetization in a stalagmite might record a larger duration of the excursion compared to marine records (Channell et al., 2020), given the accuracy of dating and the close location to the Padul site, we here take the age range for this event provided in Osete et al. (2012) using U-series. In more detail, we consider the age range between $116.5 \pm 0.7$ and $112.0 \pm 1.9$ kyr as the most accurate dating for the Blake event and applied to the Padul record between 2321 and 2277 cm. Below the main body of the excursion interval, sample BL24 (2340 cm) also shows a negative inclination and is interpreted as of reversed polarity. In addition, between 2355 cm and 2335 cm a number of samples show low-quality directions or high MAD angles. Altogether, it might indicate the presence of another magnetic excursion. This would also agree with Osete et al. (2012) who found a

short low-inclination interval before the main Blake event (119.3 ± 0.8 to 118.3 ± 0.7 kyr).

### 5.2. Reliability of some reversed polarity samples

Below the Blake interval two other intervals with negative or very low inclinations were found (Fig. 6). The first of them is located between 3860 cm and 3825 cm depth and is defined by a sample with a negative inclination (IB13, Fig. 6). However, NRM intensity for this sample is an order of magnitude above the neighboring samples, whilst no change in magnetic susceptibility is reported. The lack of a lithological change respect of samples above and below and the low magnetic susceptibility suggest that the high NRM values are not related to changes in the facies nor mineralogy. We suspect that an external factor like a lightning-induced magnetization (e.g. Platzman et al., 1998) or contamination of the plastic box could account for this anomaly. Accordingly, we did not consider the demagnetization results for polarity purposes.

### 5.3. The Iceland basin event

The interval between 4011 and 3940 cm depth, interpreted as the Iceland Basin event, is characterized by the occurrence of very low (IB24, IB25, IB29) or negative (IB27, IB28) inclination values. These samples show clear directions, but some of them (IB26, IB27, IB28) have high (>15°) MAD angles. In spite of that high MAD angles should be taken carefully, a similar behavior is reproduced in other sections embracing the Iceland Basin Interval (Channell et al., 2014). Moreover, increased MAD values are an expected feature related to the combination of a non-instantaneous acquisition of the magnetization in sediments leading to superimposed magnetization components and also as a consequence of a decreased magnetizing field intensity during the excursion intervals (e.g. Channell et al., 1997 or Lehman et al., 1996). This results into a less precise definition of magnetization components and higher MAD values during magnetic excursions (Channell et al., 2014). Accordingly, and despite the high MAD values, we interpret this interval as a reliable reversed (or low inclinations) interval, and very possibly related to a magnetic excursion.

This interval, rich in clayey carbonate and clayey peat facies sediments (and dolomite layers), has been linked to cold climate conditions with low summer evapotranspiration occurring at insolation minima times (Camuera et al., 2018). Based on cyclostratigraphy and palynology data, this interval has been attributed to MIS-6e, close to the MIS-7/6 boundary, with an age around 184 kyr (Camuera et al., 2018, 2019).

The Iceland Basin excursion is the most widely recorded geomagnetic excursions in sediments and it has been recorded several times in the Atlantic and Pacific Ocean marine sequences (Channell et al., 2014), likely favored by its long duration (Channell et al., 2020). It has, however, only been recorded in marine and lake sediment cores (Yamazaki and Yoka, 1994; Roberts et al., 1997; A.P. Roberts, 2008; Weeks et al., 1995; Channell et al., 1997, 2012, 2017; Channell, 1999, 2006; Lund et al., 2001b; Channell and Raymo, 2003; Stoner et al., 2003; Oda et al., 2002; Thouveny et al., 2004; Knudsen et al., 2006; Laj et al., 2006; Evans et al., 2007). There is a consensus of these studies placing the age of the Iceland Basin event in the 190-185 kyr range (Channell et al., 2014). At sites U1302/03 and U1306, the Iceland Basin excursion coincides closely with the MIS-7/6 boundary with the midpoint of the excursion at *ca.* 192-189 kyr (~190.2 ± 1.8 kyr). The Iceland Basin excursion would have a maximum duration of 4.96 kyr (192.7–187.7 kyr; Channell et al., 2014).

For the range of ages of the Iceland Basin event, here we follow Channell et al. (2014) *wide* scenario of VGP <40°. Assuming that this excursion is perfectly compatible with the Iceland basin event and that high MAD values prevent to exactly place the excursion in the core, we provide tentative ages for the Iceland Basin event in the Padul 15–05 core that can be helpful to future works: 4011 cm would correspond to the older limit of the excursion 192.7 kyr, while 3940 cm would correspond to 187.7 kyr.

### 5.4. Chronological implications for the Padul-15-05 record

The two new paleomagnetic dates would help constrain the timing of the oldest paleoclimatic changes registered in the Padul-15-05 sedimentary record (Fig. 7). The identification of the Iceland Basin Event increases in ~7 kyr the time interval recorded at 4010 cm depth by the previous studies (Camuera et al., 2018, 2019). In addition, using the SAR of the 4010 cm-long record and interpolated to the base of the core, the 42.64 m-long Padul-15-05 record would have recorded the last 205 kyr (MIS-7b/7a).

Our new findings show that the marine isotope substage MIS-7a, the last part of the penultimate interglacial period, between 202 and 197 kyr in the Alps (Wendt et al., 2021), is entirely registered in the Padul 15–05 core (Fig. 7). In southern Spain, this interval exhibits a gradual decrease in arboreal pollen. The geochronological results also specified an earlier occurrence of the MIS-7/6 transition, the penultimate glacial inception (~197-191 cal kyr, according to Wendt et al. (2021), than the one reported in the previous chronology of the core (Camuera et al., 2018, 2019).

The evidence of the Blake event in the Padul-15-05 record allowed the accurate constraint of the end of the Last Interglacial period, the Eemian (MIS-5e, ~115 kyr). According to the new chronological data, this key point would have occurred up to ~3 kyr later than in the previously reported chronology by Camuera et al. (2018, 2019), agreeing with the beginning of the decline of the arboreal pollen record (Camuera et al., 2019).

## 6. Conclusions

We present a high-resolution study of the magnetic stratigraphy and magnetic mineralogy for the >100kyr sedimentary succession of the Padul-15-05 core located in the southern Iberian Peninsula. We obtained the demagnetization directions for 101 samples using AF methods, and assessed the magnetic mineralogy of 5 key samples representative of the different facies. IRM acquisition experiments reveal magnetite as the main magnetic carrier. Demagnetization results show that most of the samples display positive inclinations, here interpreted as normal polarity directions. In addition, two intervals also show samples either with reliable reversed polarity or low magnetic inclinations.

The first interval prone in reversed polarity samples is located between 2321 cm and 2277 cm depth. This interval is ascribed to the Blake magnetic excursion with an oldest age of 116.5 kyr ± 0.7 kyr and a youngest age of 112 kyr ± 1.9 kyr.

The second reliable reversed interval ranges from 4011 to 3940 cm. Samples in this interval show negative or low inclinations and high MAD angles, indicating a likely magnetic excursion. Palynologic and cyclostratigraphic interpretations placed this interval slightly before of the MIS-7/6 boundary, at *ca.* 191 kyr. Accordingly, we suggest that this interval could correspond to the Iceland Basin geomagnetic event, with a maximum range of ages between 192.7 and 187.7 kyr (*wide* scenario of VGP <40°) for the interval between 4011 cm and 3940 cm depth.

The age model around the Blake interval has been refined by emplacing an age data constraint at *ca.* 116-112 kyr, confirming that the demise of the Eemian (MIS-5e) would have occurred 3 kyr later than the estimation by Camuera et al. (2018, 2019) for the same record. The identification of the Iceland Basin event also provides a very valuable time constraint at the base of the core, which would locate the MIS-7/6 transition within the 4010 to 3940 cm interval, slightly above the position provided in previous works (~7 kyr earlier) by Camuera et al. (2018, 2019). This new chronological framework has accurately specified the age of the bottom of the Padul-15-05 core at ~205 kyr.

This work provides key chronostratigraphic independent tie-points for intervals with scarce or nonexistent direct age data points, showing that the study of Earth magnetic excursions constitutes a very

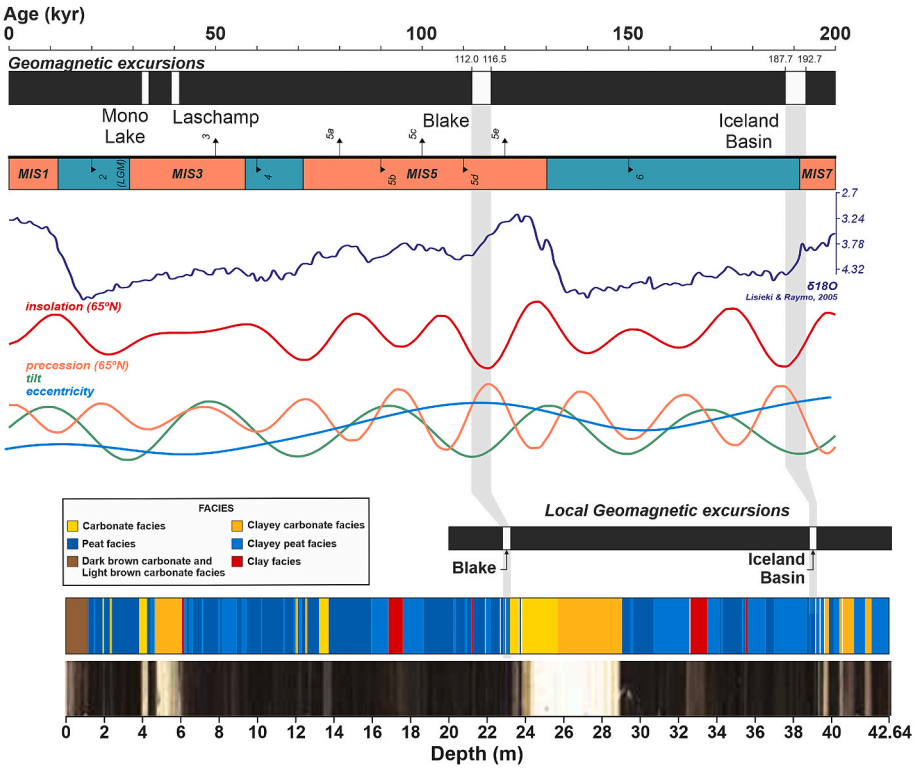


**Fig. 7.** Updated chronology for the Padul 15–05 core for sediments older than 100 kyr. From bottom to top, picture of the Padul 15–05 core and facies interpretation. Above, the magnetic excursions recorded in the core and a correlation with the geomagnetic excursion ages provided in Laj and Channel (2007; Mono Lake Laschamp), Osete et al., 2012 (Blake) and Channell et al., 2014 (Iceland Basin). Our new chronological information is compared with orbital precession, obliquity and eccentricity, and insolation (Laskar et al., 2004) and $\delta^{18}O$ values (Lisiecki and Raymo, 2005).

valuable tool to provide tie-points to constrain chronologies in time spans beyond the radiocarbon dating method.

## Declaration of competing interest

The authors declare that they have no known competing financial interests or personal relationships that could have appeared to influence the work reported in this paper.

## Data availability

Data will be made available on request.

## Acknowledgments

This study was supported by the project B-RNM-144-UGR18 and A-RNM-336-UGR20 of the action "Proyectos I + D + i del Programa Operativo FEDER 2018 - Junta de Andalucía-UGR", the projects CGL2013-47038-R and CGL2017-85415-R, of the "Ministerio de Economía y Competitividad of Spain and Fondo Europeo de Desarrollo Regional FEDER", and the research group RNM-190 (Junta de Andalucía), and the projects P18-RT-871 and Retos P20_00059 of Junta de Andalucia. A.G.-A. was also supported by a Ramón y Cajal Fellowship RYC-2015-18966 of the Spanish Government (Ministerio de Economía y Competividad). A.L.-A PhD is funded by BES-2018-084293 (Ministerio de Economía y Competividad). We thank the Paleomagnetic Laboratory CCiTUB-Geo3Bcn CSIC for the support on paleomagnetic analysis. LV and EB thank the Geomodels Research Institute (UB). We are very grateful to two anonymous reviewers and to the editor Christian Zeeden.

## References

Álvarez-Lao, D.J., Kahlke, R.D., García, N., Mol, D., 2009. The Padul mammoth finds. On the southernmost record of Mammuthus primigenius in Europe and its southern spread during the Late Pleistocene. Palaeogeogr. Palaeoclimatol. Palaeoecol. 278, 57–70. https://doi.org/10.1016/j.palaeo.2009.04.011.

An, Z.S., Kukla, G.J., Porter, S.C., Xiao, J., 1991. Magnetic susceptibility evidence of monsoon variation on the loess plateau of central China during the last 130,000 years. Quat. Res. 36, 29–36. https://doi.org/10.1016/0033-5894(91)90015-W.

Bourne, M., MacNiocaill, C., Thomas, A.L., Knudsen, M.F., Henderson, G.M., 2012. Rapid directional changes associated with a 6.5kyr-long Blake geomagnetic excursion at the Blake-Bahama Outer Ridge. Earth Planet Sci. Lett. 333, 21–34. https://doi.org/10.1016/j.epsl.2012.04.017.

Broecker, W.S., van Donk, J., 1970. Insolation changes, ice volumes, and the $^{18}O$ record in deep-sea cores. Rev. Geophys. Space Phys. 8, 169–198. https://doi.org/10.1029/RG008i001p00169.

Camuera, J., Jiménez-Moreno, G., Ramos-Román, M.J., García-Alix, A., Toney, J.L., Anderson, R.S., Jiménez-Espejo, F., Kaufman, D., Bright, J., Webster, C., Yanes, Y., Carrión, J.S., Ohkouchi, N., Suga, H., Yamame, M., Yokoyama, Y., Martínez- Ruiz, F., 2018. Orbital-scale environment and climatic changes recorded in a new ~ 200,000-year-long multiproxy sedimentary record from Padul, southern Iberian Peninsula. Quat. Sci. Rev. 198, 91–114. https://doi.org/10.1016/j.quascirev.2018.08.014.

Camuera, J., Jiménez-Moreno, G., Ramos-Román, M.J., García-Alix, A., Toney, J.L., Anderson, R.S., Jiménez-Espejo, F., Bright, J., Webster, C., Yanes, Y., Carrión, J.S., 2019. Vegetation and climate changes during the last two glacial-interglacial cycles in the western Mediterranean: a new long pollen record from Padul (southern Iberian Peninsula). Quat. Sci. Rev. 205, 86–105. https://doi.org/10.1016/j.quascirev.2018.12.013.

Camuera, J., Jiménez-Moreno, G., Ramos-Román, M.J., García-Alix, A., Jiménez-Espejo, F.J., Toney, J.L., Anderson, R.S., 2021. Chronological control and centennial-scale climatic subdivisions of the Last Glacial Termination in the western Mediterranean region. Quat. Sci. Rev. 255, 106814 https://doi.org/10.1016/j.quascirev.2021.106814.

Camuera, J., Ramos-Román, M.J., Jiménez-Moreno, G., García-Alix, A., Ilvonen, L., Ruha, L., Gil-Romera, G., González-Sampériz, P., Seppä, H., 2022. Past 200 kyr hydroclimate variability in the western mediterranean and its connection to the african humid periods. Sci. Rep. 12, 1–13. https://doi.org/10.1038/s41598-022-12047-1.

Channell, J.E.T., 1999. Geomagnetic paleointensity and directional secular variation at ocean drilling program (ODP) site 984 (bjorn drift) since 500 ka: comparisons with ODP site 983 (gardar drift). J. Geophys. Res. 104, 22937–22951. https://doi.org/10.1029/1999JB900223.

Channell, J.E.T., 2006. Late brunhes polarity excursions (Mono Lake, Laschamp, Iceland basin and pringle falls) recorded at ODP site 919 (irminger basin). Earth Planet Sci. Lett. 244, 378–393. https://doi.org/10.1016/j.epsl.2006.01.021.

Channell, J.E.T., Raymo, M.E., 2003. Paleomagnetic record at ODP site 980 (feni drift, rockall) for the past 1.2 myrs. G-cubed 4, 1033. https://doi.org/10.1029/2002GC000440.

Channell, J.E.T., Hodell, D.A., Lehman, B., 1997. Relative geomagnetic paleointensity and $\delta^{18}O$ at ODP site 983 (gardar drift, north atlantic) since 350 ka. Earth Planet Sci. Lett. 153, 103–118. https://doi.org/10.1016/S0012-821X(97)00164-7.

Channell, J.E.T., Hodell, D.A., Curtis, J.H., 2012. ODP Site 1063 (Bermuda Rise) revisited: oxygen isotopes, excursions and paleointensity in the Brunhes Chron. G-cubed 13, Q02001. https://doi.org/10.1029/2011GC003897.

Channell, J.E.T., Wright, J.D., Mazaud, A., Stoner, J.S., 2014. Age through tandem correlation of Quaternary relative paleointensity (RPI) and oxygen isotope data at IODP Site U1306 (Eirik Drift, SW Greenland). Quat. Sci. Rev. 88, 135e146. https://doi.org/10.1016/j.quascirev.2014.01.022.

Channell, J.E.T., Vázquez Riveiros, N., Gottschalk, J., Waelbroeck, C., Skinner, L.C., 2017. Age and duration of Laschamp and Iceland Basin geomagnetic excursions in the south atlantic ocean. Quat. Sci. Rev. 167, 1e13. https://doi.org/10.1016/j.quascirev.2017.04.020.

Channell, J.E., Singer, B.S., Jicha, B.R., 2020. Timing of Quaternary geomagnetic reversals and excursions in volcanic and sedimentary archives. Quat. Sci. Rev. 228, 106114 https://doi.org/10.1016/j.quascirev.2019.106114.

Creer, K.M., Readman, P.W., Jacobs, A.M., 1980. Palaeomagnetic and palaeontological dating of a section at gioia tauro, Italy: identification of the Blake event. Earth Planet Sci. Lett. 50, 289–300. https://doi.org/10.1016/0012-821X(80)90139-9.

Denham, C.R., 1976. Blake polarity episode in two cores from the Greater Antilles outer ridge. Earth Planet Sci. Lett. 29, 422–443. https://doi.org/10.1016/0012-821X(76)90147-3.

Denham, C.R., Cox, A., 1971. Evidence that the Laschamp polarity event did not occur 13,300-34,000 years ago. Earth Planet Sci. Lett. 13, 181–190. https://doi.org/10.1016/0012-821X(71)90122-1.

Domingo-García, M., Fernández-Rubio, R., López-González, J.D., González- Gómez, C., 1983. Aportación al conocimiento de la neotectónica de la depresión de Padul (Granada). Rev. Esp. Geol. Min. 53, 6–16.

Evans, H.F., Channell, J.E.T., Stoner, J.S., Hillaire-Marcel, C., Wright, J.D., Neitzke, L.C., Mountain, G.S., 2007. Paleointensity-assisted chronostratigraphy of detrital layers on the Eirik Drift (North Atlantic) since marine isotope stage 11. G-cubed 8, Q11007. https://doi.org/10.1029/2007GC001720.

Fang, X., Li, J., Van der Voo, R., MacNiocaill, C., Dai, X., Kemp, R.A., Derbyshire, E., Cao, J., Wang, J., Wang, G., 1997. A record of the Blake Event during the last interglacial paleosol in the western loess plateau of China. Earth Planet Sci. Lett. 146, 73–82. https://doi.org/10.1016/S0012-821X(96)00222-1.

Florschutz, F., Menéndez-Amor, J., Wijmstra, T.A., 1971. Palynology of a thick Quaternary succession in southern Spain. Palaeogeogr. Palaeoclimatol. Palaeoecol. 10, 233–264. https://doi.org/10.1016/0031-0182(71)90049-6.

Garcia-Alix, A., Jimenez-Moreno, G., Anderson, R.S., Espejo, F.J.J., Huertas, A.D., 2012. Holocene environmental change in southern Spain deduced from the isotopic record of a high-elevation wetland in Sierra Nevada. J. Paleolimnol. 48, 471–484. https://doi.org/10.1007/s10933-012-9625-2.

García-Alix, A., Camuera, J., Ramos-Román, M.J., Toney, J.L., Sachse, D., Schefuß, E., Jiménez-Moreno, G., Jiménez-Espejo, F.J., López-Avilés, A., Anderson, R.S., Yanes, Y., 2021. Paleohydrological dynamics in the Western Mediterranean during the last glacial cycle. Global Planet. Change 202, 103527. https://doi.org/10.1016/j.gloplacha.2021.103527.

Gómez-Ortiz, A., Schulte, L., Salvador Franch, F., Palacios Estremera, D., Sanz de Galdeano, C., Sanjosé Blasco, J.J., Tanarro García, L.M., Atkinson, A., 2005. The Geomorphological Unity of the Veleta: a Particular Area of the Sierra Nevada Guidebook. Sixth International Conference of Geomorphology, Zaragoza.

Knudsen, M.F., Mac Niocaill, C., Henderson, G.M., 2006. High-resolution data of the Iceland Basin geomagnetic excursion from ODP sites 1063 and 983: existence of intense flux patches during the excursion? Earth Planet Sci. Lett. 251, 18–32. https://doi.org/10.1016/j.epsl.2006.08.016.

Laj, C., Channell, J.E.T., 2007. Geomagnetic excursions. In: Kono, M. (Ed.), Treatise on Geophysics. Geomagnetism 5, 373–416. https://doi.org/10.1016/B978-044452748-6.00095-X (Chapter 10). Elsevier, Amsterdam 2007.

Laj, C., Kissel, C., Roberts, A.P., 2006. Geomagnetic field behavior during the Icelandic basin and Laschamp geomagnetic excursions: a simple transitional field geometry? G-cubed 7, Q03004. https://doi.org/10.1029/2005GC001122.

Laskar, J., Robutel, P., Joutel, F., Gastineau, M., Correia, A.C.M., Levrard, B., 2004. A long-term numerical solution for the insolation quantities of the Earth. Astron. Astrophys. 428, 261–285. https://doi.org/10.1051/0004-6361:20041335.

Lehman, B., Laj, C., Kissel, C., Mazaud, A., Paterne, M., Labeyrie, L., 1996. Relative changes of the geomagnetic field intensity during the last 280 kyear from piston cores in the Azores area. Phys. Earth Planet. In. 93, 269–284. https://doi.org/10.1016/0031-9201(95)03070-0.

Lisiecki, L.E., Raymo, M.E., 2005. A Pliocene-Pleistocene stack of 57 globally distributed benthic δ18O records. Paleoceanography 20. https://doi.org/10.1029/2004PA001071.

Lund, S.P., Acton, G.D., Clement, B., Okada, M., Williams, T., 2001. Paleomagnetic records of stage 3 excursions, leg 172. In: Keigwin, L.D., Rio, D., Acton, G.D., Arnold, E. (Eds.), Proceedings of the ODP Science Research 172, 1–20.

Lund, S.P., Stoner, J.S., Channell, J.E.T., Acton, G., 2006. A summary of Brunhes paleomagnetic field variability recorded in Ocean Drilling Program cores. Phys. Earth Planet. In. 156, 194–204. https://doi.org/10.1016/j.pepi.2005.10.009.

Menéndez-Amor, J., Florschutz, F., 1962. Un aspect de la végétation en Espagne méridionale durant la dernière glaciation et L'Holocène. Geol. Mijnbouw 41, 131–134.

Menéndez-Amor, J., Florschutz, F., 1964. Results of the preliminary palynological investigation of samples from a 50 m boring in southern Spain. Bol. R. Soc.Esp. His. Nat. 62, 251–255.

Nestares, T., Torres, T., 1998. Unnuevo sondeo de investigacion paleoambiental del Pleistocenoy Holoceno en la turbera de Padul (Granada, Andalucía). Geogaceta 23, 99–102.

Oda, H., Nakamura, K., Ikehara, K., Nakano, T., Nishimura, M., Khlystov, O., 2002. Paleomagnetic record from Academician ridge, Lake Baikal: a reversal excursion at the base of marine oxygen isotope stage 6. Earth Planet Sci. Lett. 202, 117–132. https://doi.org/10.1016/S0012-821X(02)00755-0.

Ortiz, J.E., Torres, T., Delgado, A., Julià, R., Lucini, M., Llamas, F.J., Resyes, E., Soler, V., Valle, M., 2004. The palaeoenvironmental and palaeohydrological evolution of Padul Peat Bog (Granada, Spain) over one million years, from elemental, isotopic and molecular geochemical proxies. Org. Geochem. 35, 1243–1260. https://doi.org/10.1016/j.orggeochem.2004.05.013.

Ortiz, J.E., Torres, T., Delgado, A., Llamas, J.F., Soler, V., Valle, M., Julià, R., Moreno, L., Díaz-Bautista, A., 2010. Palaeoenvironmental changes in the Padul basin (Granada, Spain) over the last 1 Ma based on the biomarker content. Palaeogeogr. Palaeoclimatol. Palaeoecol. 298, 286–299. https://doi.org/10.1016/j.palaeo.2010.10.003.

Osete, M.-L., Martin-Chivelet, J., Rossi, C., Edwards, R.L., Egli, R., Muñoz-García, M.B., Wang, X., Pavón-Carrasco, F.J., Heller, F., 2012. The Blake geomagnetic excursion recorded in a radiometrically dated speleothem. Earth Planet Sci. Lett. 353, 173–181. https://doi.org/10.1016/j.epsl.2012.07.041.

Palacios, D., Gómez-Ortiz, A., Andrés, N., Salvador, F., Oliva, M., 2016. Timing and new geomorphologic evidence of the last deglaciation stages in Sierra Nevada (southern Spain). Quat. Sci. Rev. 150, 110e129. https://doi.org/10.1016/j.quascirev.2016.08.012.

Pancost, R.D., 2017. Climate change narratives. Nat. Geosci. 10, 466–468. https://doi.org/10.1038/ngeo2981.

Parés, J.M., Van Der Voo, R., Yan, M., Fang, X., 2004. After the dust settles: why is the Blake Event imperfectly recorded in Chinese Loess? Geophys. Monogr. 145, 191–204. https://doi.org/10.1029/145GM14.

Platzman, E.S., Tapirdamaz, C., Sanver, M., 1998. Neogene anticlockwise rotation of central Anatolia (Turkey): preliminary palaeomagnetic and geochronological results. Tectonophysics 299, 175–189. https://doi.org/10.1016/S0040-1951(98)00204-2.

Pons, A., Reille, M., 1988. The Holocene- and upper Pleistocene pollen record from Padul (Granada, Spain): a new study. Palaeogeogr. Palaeoclimatol. Palaeoecol. 66, 243–263. https://doi.org/10.1016/0031-0182(88)90202-7.

Ramos-Román, M.J., Jiménez-Moreno, G., Camuera, J., García-Alix, A., Anderson, R.S., Jiménez-Espejo, F.J., Carrión, J.S., 2018a. Holocene climate aridification trend and human impact interrupted by millennial-and centennial-scale climate fluctuations from a new sedimentary record from Padul (Sierra Nevada, southern Iberian Peninsula). Clim. Past 14, 117–137. https://doi.org/10.5194/cp-14-117-2018.

Ramos-Román, M.J., Jiménez-Moreno, G., Camuera, J., García-Alix, A., Anderson, R.S., Jiménez-Espejo, F.J., Sachse, D., Toney, J., Carrión, J.S., Webster, C., Yanes, Y., 2018b. Millennial-scale cyclical environment and climate variability during the Holocene in the western Mediterranean region deduced from a new multi- proxy analysis from the Padul record (Sierra Nevada, Spain). Global Planet. Change 168, 35–53. https://doi.org/10.1016/j.gloplacha.2018.06.003.

Roberts, A.P., 2008. Geomagnetic excursions: knowns and unknowns. Geophys. Res. Lett. 35, L17307 https://doi.org/10.1029/2008GL034719.

Roberts, A.P., 2008. Geomagnetic excursions: knowns and unknowns. Geophys. Res. Lett. 35, L17307 https://doi.org/10.1029/2008GL034719.

Roberts, A.P., Lehman, B., Weeks, R.J., Verosub, K.L., Laj, C., 1997. Relative paleointensity of the geomagnetic field over the last 200,000 years from ODP Sites 883 and 884, north Pacific ocean. Earth Planet Sci. Lett. 52, 11–23. https://doi.org/10.1016/S0012-821X(97)00132-5.

Rodrigo-Gámiz, M., García-Alix, A., Jiménez-Moreno, G., Ramos-Román, M.J., Camuera, J., Toney, J.L., Sachse, D., Anderson, R.S., Damsté, J.S.S., 2022. Paleoclimate reconstruction of the last 36 kyr based on branched glycerol dialkyl glycerol tetraethers in the Padul palaeolake record (Sierra Nevada, southern Iberian Peninsula). Quat. Sci. Rev. 281, 107434 https://doi.org/10.1016/j.quascirev.2022.107434.

Schulte, L., 2002. Climatic and human influence on river systems and glacier fluctuations in southeast Spain since the Last Glacial Maximum. Quat. Int. 93–94, 85–100. https://doi.org/10.1016/S1040-6182(02)00008-3.

Singer, B.S., Guillou, H., Jicha, B.R., Zanella, E., Camps, P., 2014. Refining the Quaternary geomagnetic instability time scale (GITS): lava flow recordings of the Blake and Post-Blake excursions. Quat. Geochronol. 21, 16–28. https://doi.org/10.1016/j.quageo.2012.12.005.

Smith, J.D., Foster, J.H., 1969. Geomagnetic reversal in the Brunhes normal polarity epoch. Science 163, 565–567. https://doi.org/10.1126/science.163.3867.565.

Stoner, J.S., Channell, J.E.T., Hodell, D.A., Charles, C., 2003. A 580 kyr paleomagnetic record from the sub-Antarctic south Atlantic (ODP Site 1089). J. Geophys. Res. 108, 2244. https://doi.org/10.1029/2001JB001390.

Thouveny, N., Carcaillet, J., Moreno, E., Leduc, G., Nerini, D., 2004. Geomagnetic moment variation and paleomagnetic excursions since 400 kyr BP; a stacked record from sedimentary sequences of the Portuguese margin. Earth Planet Sci. Lett. 219, 377–396. https://doi.org/10.1016/S0012-821X(03)00701-5.

Torres, T., Valle, M., Ortiz, J.E., Soler, V., Araujo, R., Rivas, M.R., Delgado, A., Julià, R., Sánchez-Palencia, Y., 2020. 800 ka of Palaeoenvironmental changes in the Southwestern Mediterranean realm. J. Iber. Geol. 46, 117–144. https://doi.org/10.1007/s41513-020-00123-2.

Tric, E., Laj, C., Valet, J.-P., Tucholka, P., Paterne, M., Guichard, F., 1991. The Blake geomagnetic event: transition geometry, dynamical characteristics and geomagnetic significance. Earth Planet Sci. Lett. 102, 1–13. https://doi.org/10.1016/0012-821X(91)90013-8.

Tucholka, P., Fontugne, M., Guichard, F., Paterne, M., 1987. The Blake polarity episode in cores from the Mediterranean Sea. Earth Planet Sci. Lett. 86, 320–326. https://doi.org/10.1016/0012-821X(87)90229-9.

Verosub, K.L., 1982. Geomagnetic excursions: a critical assessment of the evidence as recorded in sediments of the Brunhes Epoch. Philos. Trans. Royal Soc. A Math. Phys. *Engen. Sci.* 306, 161–168. https://doi.org/10.1098/rsta.1982.0076, 1492.

Weeks, R.J., Laj, C., Endignoux, L., Mazaud, A., Labeyrie, L., Roberts, A.P., Kissel, C., Blanchard, E., 1995. Normalized NRM intensity during the last 240,000 years in piston cores from the central north Atlantic ocean: geomagnetic field intensity or environmental signal? Phys. Earth Planet. In. 87, 213–229. https://doi.org/10.1016/0031-9201(94)02966-F.

Wendt, K.A., Li, X., Edwards, R.L., Cheng, H., Spötl, C., 2021. Precise timing of MIS 7 substages from the Austrian Alps. Clim. Past 17, 1443–1454. https://doi.org/10.5194/cp-17-1443-2021.

Yamazaki, T., Yoka, N., 1994. Long-term secular variation of the geomagnetic field during the last 200 kyr recorded in sediment cores from the western equatorial Pacific. Earth Planet Sci. Lett. 128, 527–544. https://doi.org/10.1016/0012-821X(94)90168-6.

Zhu, R.X., Zhou, L.P., Laj, C., Mazaud, A., Ding, D.L., 1994. The Blake geomagnetic polarity episode recorded in Chinese loess. Geophys. Res. Lett. 21, 697–700. https://doi.org/10.1029/94GL00532.